

# Stand age and species composition effects on surface albedo in a mixedwood boreal forest

Mohammad Abdul Halim<sup>1,2</sup>, Han Y. H. Chen<sup>3</sup>, Sean C. Thomas<sup>1</sup>

<sup>1</sup>University of Toronto, Faculty of Forestry, 33 Willcocks Street, M5S 3B3, ON, Canada

<sup>2</sup>Shahjalal University of Science and Technology, Dept. of Forestry and Environmental Science, Sylhet-3114, Bangladesh

<sup>3</sup>Lakehead University, Natural Resources Management, 955 Oliver Road, Thunder Bay, P7B 5E1, ON, Canada

*Correspondence to:* Mohammad Abdul Halim (abdul.halim@mail.utoronto.ca)

**Abstract.** Surface albedo is one of the most important processes governing climate forcing in the boreal forest and is directly affected by management activities such as harvesting and natural disturbances such as forest fires. Empirical data on the effects of these disturbances on boreal forest albedo are sparse. We conducted ground-based measurements of surface albedo from a series of instrument towers over four years in a replicated chronosequence of mixedwood boreal forest sites differing in stand age (year since disturbance) in both post-harvest and post-fire stands. We investigated the effects of stand age, canopy height, tree species composition, and ground vegetation cover on surface albedo through stand development. Our results indicate that winter (0-19 years) and spring (7-19 years) albedo values were 63 and 24 % higher, respectively, in post-harvest stands than in post-fire stands. Summer and fall albedo values were similar between disturbance types, with summer albedo showing a transient peak at ~10 years stand age. Winter and summer albedos saturated at roughly 50 years stand age in both post-harvest and post-fire stands. The proportion of deciduous broadleaf species showed a strong positive relationship with seasonal averages of albedo in both post-harvest and post-fire stands. Given that stand composition in mixedwood boreal forests generally shows a gradual replacement of deciduous trees by conifers, our results suggest that successional changes in species composition are likely a key driver of age-related patterns in albedo. Our findings also suggest the efficacy of increasing the proportion of deciduous broadleaf species as a silvicultural option for climate-friendly management of the boreal forest.

## Keywords

Stand age, species composition, canopy height, ground vegetation cover, harvesting, forest fire, succession, surface albedo, boreal forest.

## 1 Introduction

Surface albedo, the fraction of incoming solar energy reflected from the surface in all directions, is one of the most important biophysical factors affecting both local and global climates. In boreal forest, the magnitude of albedo-related forcing on climate is even more important than in other ecosystems because of snow-related feedbacks, low sensible heat flux, and the relative stability of the atmospheric temperature profile due to weak latent-heat-driven convection (Bright et al., 2015a; Hansen et al., 2005). Even though albedo is increasingly used as an important state variable in climate models (Brown and Caldeira, 2017; Bala et al., 2007; Betts, 2000), forest disturbance effects on net radiative forcing due to local albedo changes and related feedbacks with regional/global mean surface temperature remain highly uncertain (Bright et al.,

2015a; Lee et al., 2011). Harvest and fire suppression may differ substantially in their effects on albedo, but empirical data on albedo responses to disturbance type remain particularly sparse.

40

Following disturbance events, albedo of boreal forests is expected to change with stand age due to changing surface properties, and forest structure and composition. Age-related stand structural attributes (e.g., tree species composition, leaf area index [LAI], canopy height, and ground vegetation cover) can substantially influence surface albedo of a stand throughout the year. Studies have generally found higher albedos in young stands than in mature stands in the boreal forest (Bright et al., 2015a; Kuusinen et al., 2014; Amiro et al., 2006b), and it has been suggested that albedo stabilizes ~ 25 years after a disturbance event (during the 'stem exclusion' phase in the ecological succession trajectory). Early in stand development boreal mixedwood forests are commonly dominated by deciduous broadleaf species (Madoui et al., 2015; Brassard and Chen, 2010; Johnstone et al., 2010), which have higher leaf and canopy reflectance than conifers (Lukeš et al., 2013a; Linacre, 2003), contributing to high summer albedo in young stands (Lukeš et al., 2013b; Betts and Ball, 1997). These deciduous species shed leaves in the winter, which increases canopy openness (lowers LAI) and allows snow albedo to dominate, contributing to the high winter albedo in young stands. Available data suggest that at this stage both LAI and ground vegetation cover usually increase with stand age, depending on site quality and silvicultural practices (Amiro et al., 2006b; Uotila and Kouki, 2005). Low LAI can increase canopy background reflectance both in snow-covered and snow-free conditions, and thus can contribute to the high albedos in young stands (Amiro et al., 2006b). LAI effects on albedo in young stands may be highly modulated by ground vegetation cover in the summer, but probably not much in the winter as ground vegetation is generally leafless or covered with snow (Kuusinen et al., 2015; Lukeš et al., 2013b; Betts and Ball, 1997). In conjunction with other factors, surface albedo tends to decrease with increasing canopy height (Hovi et al., 2016; Linacre, 2003). In the later stages of stand development, albedo is expected to saturate non-linearly as conifers dominate the stand and canopy cover and stand attributes change gradually, but data describing this pattern remain sparse (Amiro et al., 2006b).

60

Harvesting and fire are the major stand-replacing disturbances in the boreal forest (Brassard et al., 2008). These disturbances may differentially affect surface albedo of post-disturbance stands in complex ways by altering ground surface spectral properties, species composition, and stand structure (Lukeš et al., 2013b; Liu et al., 2005), but field data directly addressing this issue are essentially limited to a single study in Europe (Kuusinen et al., 2016). Structure and composition of post-fire stands are generally more heterogeneous than post-harvest stands; for example, post-fire stands are more likely to show a bimodal vertical structure and a mixture of conifer and hardwood species during early stand development stages (Brassard and Chen, 2010; Chen et al., 2009). Charcoal residues may also strongly reduce albedo in snow-free conditions in the first years following fire disturbances (Amiro et al., 2006b). Both charcoal effects and stand heterogeneity might be expected to reduce surface albedo in post-fire stands relative to post-harvest stands. However, the magnitude of this difference in surface albedo might be less than expected due to the presence of legacy charcoals from historical fires in post-harvest stands (Hart and Luckai, 2013). Immediately after harvesting, the albedo of a post-harvest stand can also be reduced because of the presence of coarse woody debris (CWD) and high soil moisture content (Linacre, 2003). In the years following a disturbance event, CWD might be expected to further reduce albedo by becoming darker in color due to decomposition processes (Brassard and Chen, 2008) and plant colonization (Kumar et al., 2018).

75

80 Despite the important roles of stand age, and stand structure and composition as determinants of boreal forest albedo, field measurements are scarce (Kuusinen et al., 2014) and particularly limited for early stand ages that show high variability in surface properties (Bright et al., 2013). This has contributed to poorly constrained estimates of the local albedo changes on net global radiative forcing (Bright et al., 2015a). Although some recent studies (e.g., Luyssaert et al., 2018; Naudts et al., 2016) have incorporated vegetation structure and composition in albedo estimation for land surface models, scarcity of field measurements is still a challenge for proper attribution of boreal forest albedo in climate models (Li et al., 2016; Thackeray et al., 2019). Thus, to estimate the net change in surface temperature as a function of albedo change from deforestation in boreal forests, a number of climate models (e.g., Bala et al. 2007, Betts 2000) have used a 'biome replacement' approach (replacing boreal forests with grassland or agricultural land cover types) and approximated boreal forests' albedo as a single value from mature stands (~ 60-year old). Early stand dynamics is reported to determine which mechanism, albedo vs. carbon storage, dominates the net forcing for the boreal forest (Kirschbaum et al., 2011). Such simplifications in climate models that do not explicitly consider stand age and successional effects on albedo will likely result in strongly biased estimations of boreal forests' albedo over the rotation (harvesting/fire) period (Bright et al., 2018).

90 Given the complex nature and limited understanding of underlying processes (Lukeš et al., 2013b), it is important to conduct field studies to better quantify forest albedo in relation to stand age and disturbance type in boreal forests. Deeper understanding of the local mechanisms that account for variation in albedo will not only enhance global climate models (e.g., by improving the land-surface model: Bright et al., 2018), but also help to design climate-friendly silvicultural practices (Astrup et al., 2018; Matthies and Valsta, 2016; Bright et al., 2015a). In the present study, we set up micrometeorological towers with pyranometers in a replicated chronosequence of post-harvest and post-fire sites to study stand age, disturbance type, and species composition effects on albedo in a mixedwood boreal forest of northwestern Ontario, Canada. We hypothesized: (1) that post-fire stands would show lower albedo values than post-harvest stands as a consequence of stand composition, legacy structures, and fire residues; (2) that all stands would approach albedo values similar to mature stands within ~ 25 years, soon after crown closure; and (3) that stands with higher dominance of deciduous broadleaf species would show higher albedo than conifer-dominated stands, with this effect being most pronounced under snow-covered conditions.

## 2 Materials and Methods

### 2.1 Study area

105 The study was conducted in the boreal forest of the Lake Nipigon region (49.55° N and 89.5° W), Ontario, Canada, approximately 200 km north of Thunder Bay. A series of circular (10-m radius) chronosequence plots were established in the post-harvest (full-tree harvest) and post-fire stands in the study area. Three plots were set up in each of three cutblocks (in separate stands) harvested in 1998, 2006, and 2013. Selected stands were at least 5 ha in size, and plots were established at least 100 m from any older or taller stand to avoid edge effects. Recent (2013) post-fire stands were not present, so we set up three plots only in post-fire stands dating from 1998 and 2006 fire events (Fig. 1). Replicate stands were spatially interspersed to the extent feasible. For each of the 15 plots, albedo and stand attributes (stand age, percentage of deciduous broadleaf species, canopy height, and percentage of ground vegetation cover) were measured from July 2013 to June 2017.

115 The mesic mixedwood study area is dominated by jack pine (*Pinus banksiana* Lamb.), black spruce (*Picea mariana* (Mill.)  
BSP), white spruce (*P. glauca* (Moench) Voss), trembling aspen (*Populus tremuloides* Michx.), eastern white cedar (*Thuja*  
*occidentalis* L.), balsam fir (*Abies balsamea* (L.) Mill.), and paper birch (*Betula papyrifera* Marsh.) (Chen and Popadiouk,  
2002). The management regime in the region is based on clearcut silviculture modified to include live tree retention in  
120 harvested stands (OMNRF, 2015); typical rotation lengths are 80 years (Colombo et al., 2005). In study plots over the study  
period canopy height ranged from 0–7.7 m, ground vegetation cover ranged from 1.8–96.7 %, LAI ranged from 0–2.1, and  
the proportion of deciduous broadleaf basal area ranged from 10.6–100 %, and stand density range from 0–11556 stem/ha  
(Table 1). The study area has an average elevation of 416 m a.s.l. The soil is a moderately deep Brunisol (coarse-loamy  
texture) with 1–15 cm thick organic layer (i.e., the total litter, fermented, and humic [LFH] layers). The area remains snow  
covered for 5–6 months with an average snow depth of ~ 10 cm (Environment Canada, 2018; Sims et al., 1997) and the  
mean annual air temperature of the study plots was  $-1.1$  °C (Halim and Thomas, 2018).

125

## 2.2 Experimental setup

In the center of each circular plot a pair of upward- and downward-facing pyranometers (Silicon [Si] pyranometer; Onset,  
Massachusetts, USA; measurement range 0–1280  $\text{Wm}^{-2}$  over a spectral range of 300–1100 nm, accuracy  $\pm 5$  %, resolution  
1.25  $\text{Wm}^{-2}$ ) were set up on a mast 3.5 m above the canopy (above the ground for 2013 post-harvest stands) to measure  
130 incident and reflected solar radiation every 10 minute. The plot and tower locations were selected to avoid trees from  
surrounding stands falling within the footprints of the pyranometers or blocking incoming solar radiation. Instrument masts  
consisted of extendible galvanized steel poles and were set in concrete bases and guyed to mitigate instrument sway. At  
least once a year pyranometer heads were cleaned and realigned to make sure they were normal to the ground. Average  
daily albedo was calculated as the ratio of daily total incident and reflected radiation for each plot. The average daily albedo  
135 was used to calculate average monthly albedo, which was finally used to calculate mean seasonal albedo for each year in  
each plot.

Quality control for the irradiance and reflected solar radiation measurements was conducted following guidelines of the  
World Meteorological Organization (WMO). Any unusually high/low values were replaced by interpolated values by taking  
140 the average of preceding and subsequent measurements. Daily total irradiance data were compared against the WMO-  
provided maximum possible daily sums of clear-sky irradiance for 50°N latitudes (WMO, 1987, p.26). If measured the daily  
total irradiance was higher than the maximum possible value, we excluded the measurements for that day. For reflected  
solar radiation, if the daily total of reflected solar radiation was higher than the daily total irradiance, we also excluded the  
measurements for that day. In addition, we excluded measurements for any snowy day; snowfall was detected using data  
145 from the closest available weather station (Environment Canada, 2018).

In addition to albedo, winter (December–February)/spring (March–May) and summer (June–August)/fall (September–  
November) proportion of deciduous broadleaf area (%), canopy height (m), and ground vegetation cover (%) were  
measured every year in late October and early July, respectively, in each plot. The proportion of deciduous broadleaf  
150 species (%) were determined for trees with diameter at breast height  $\geq 5$  cm and height  $> 1$  m. Canopy height was  
determined as the mean height of all trees sampled; the young stands sampled were at stages of development prior to and  
just after canopy closure, so essentially all trees were “canopy dominants”. The proportion of deciduous broadleaf species of

a plot was calculated as the ratio of basal area of the deciduous species to the total basal of area of the plot. In each plot, four 1-m<sup>2</sup> subplots were set up and percent ground vegetation cover was determined visually (Kumar et al., 2018). Stand age was determined as the time (year) since the last disturbance (fire/harvesting) for each plot. Fire maps (from the Ontario Ministry of Natural Resources, Canada) and forest management plans (from Resolute Forest Products, Canada) were used to verify type and year of disturbances.

### 2.3 Sources of secondary data

Since we did not have recent post-fire stands (0–6-year old) in the study area, we used secondary albedo data from studies in post-fire boreal forests with similar stand characteristics in Saskatchewan and Manitoba (Canada) (Fig. 1). We also used secondary albedo data for old stands (> 70 years) from these sites along with primary data to develop regression models for both post-fire and post-harvest stands. Here we assumed that at this stage of stand development, there is negligible difference in stand attributes (e.g., species composition, height, LAI) between post-fire and post-harvest stands (Moussaoui et al., 2016). We did not use satellite-based albedo data as secondary sources as they tend to diverge from field measurements depending on a number of factors including stand age, latitude, and cloud cover effects (Halim and Thomas, 2017; Bright et al., 2015b).

Data for Saskatchewan sites were retrieved from Amiro et al. (2006a), and for Manitoban sites from Amiro et al., (2006b) by digitizing data points from relevant figures using the WebPlotDigitizer software (Rohatgi, 2018). These stands were dominated by jack pine and black spruce with some intermixing of trembling aspen. All post-fire sites (including this study) had severe fires that completely killed previous vegetations. There were a few burned snags in the Saskatchewan and Manitoban sites and none in the present study sites. These areas remain snow covered for ~ 6 months with average snow depths of 10–15 cm (Environment Canada, 2018). Pyranometers were located in Saskatchewan sites at 18–20 m, and in Manitoban sites at 6 m heights. There was no detailed information on how proportions of broadleaf deciduous species were calculated for these sites; however, we assumed they were basal-area based. A detailed description of the study areas and methods can be found in the respective articles.

### 2.4 Accuracy assessment of albedo measurements

To test the relative accuracy of albedo measurements from Si-based pyranometers (Onset Computers' Hobo, used in this study) in comparison to thermopile pyranometers (Kipp and Zonen's CNR1, used in the studies providing secondary data), we conducted a field calibration study over nine days under variable sky and ground conditions (see Supplementary Materials). Results from this study showed a very close agreement between the measurements of Hobo and CNR1 pyranometers (Fig. S1). The difference (CNR1 – Hobo) in daily albedo over the study period ranged from – 0.0601 to 0.064, and the mean difference in daily albedo was 0.0028 ( $\pm$  0.031). The mean difference was negligible and the range in differences was well within the previously reported error ranges (~ 5–7 %) for similar pyranometers (Myers, 2010; Stroeve et al., 2005). We also did not observe any detectable pattern in deviations between the pyranometers under different sky and ground conditions. We therefore concluded that albedo measurements from Si-based Hobo and thermopile-based CNR1 pyranometers are closely comparable, and corrections to the Si-based albedo estimates presented are not warranted.

## 2.5 Measurements of ground surface reflectance

To examine effects of disturbance type on ground surface reflectance, three soil samples (top 10 cm including LFH layer, surface area 78.5 cm<sup>2</sup>) from each plot were collected in fall 2017 to measure the ground surface reflectance. Samples were all collected within a two-day precipitation-free period, and were brought to the lab in airtight packaging without disturbing the top surface. A spectrometer (SD 2000; Ocean Optics, Florida, USA; measurement spectral range 338.7–1001.8 nm) equipped with an integrating sphere was used to measure the directional-hemispherical reflectance factor of the top surface of the soil samples. As there were no recent post-fire stands in the study area, we collected charcoal samples (of twigs, branches, barks, and stems) from the forest floor of a jack pine dominated post-fire (fire occurred in 2011) stand in summer 2015 from near the Musselwhite mine (52.61° N and 90.37° W), Ontario, Canada. Every sample was measured ten times in ten different locations (each 0.84 cm<sup>2</sup> in area), and each measurement was performed by scanning 10 times (with Boxcar width 5 [spatial averaging of 5 pixels] and 100 millisecond integration time) to get an average reflectance for each location of a sample. Details of the spectrometer and integrating sphere used can be found in the Materials and Methods section of Baltzer and Thomas (2005). Forest floor reflectance values from the Musselwhite stand (4-year old) were compared to soil sample reflectance values from recent (2013) post-harvest stands (4-year old). For older stands (1998 and 2006 post-harvest and post-fire stands), soil sample reflectance data were compared using samples from the main study plots.

## 2.6 Data analysis

Robust t-tests (Wilcox, 2016) were used to compare mean differences in ground surface reflectance (in visible [400–700 nm] and near-infrared [ $> 700$ –1000 nm] spectral bands) and seasonally averaged albedo between post-harvest and post-fire stands. Mean seasonal albedo values of post-harvest and post-fire stands were also compared using Analysis of Covariance (ANCOVA) controlling for the effects of stand age as a covariate. Secondary albedo data for 0–6-year-old post-fire stands were only available for winter and summer seasons. Therefore, in the t-tests (and in ANCOVA) for winter and summer albedo, data from 0–19-year old post-harvest and post-fire stands were used. For spring and fall, albedo data from recent (0–6-year-old) post-harvest stands were omitted (since there were no data from post-fire stands for these seasons), and data from 7–19-year-old stands were used to make the comparisons unbiased. Secondary data from old stands ( $> 70$  years) were not used in the t-tests/ANCOVA. These analyses treat seasonally averaged albedo values from the same stands as independent. We also conducted parallel analyses using linear mixed models that included plot as a random variable; in all cases, the random effect was not significant, and thus only the simpler linear model results are presented.

Generalized linear models (GLMs) with the log-linked gaussian family (additive-observation-error model with constant variance) were found to be the best fitted to model seasonal albedo as a function of stand attributes (stand age, proportion of deciduous broadleaf species, canopy height, ground vegetation cover, and their interactions) for both post-harvest and post-fire stands. Best models were chosen using an AIC-based stepwise algorithm. Asymptotic chi-square statistics based on deviance were calculated for each best-fit model to test if the model was significantly better than its counterpart null model. In fall months, some stand attributes were only nonlinearly (double exponentially) related to albedo. To avoid model complexity, for each of these fall attributes a separate nonlinear model was fitted, and for other attributes GLMs with identity-linked gaussian family were found to be the most suitable. The  $\Delta$ AIC for each best-fit model is calculated as its AIC difference with the corresponding null model (AIC of the best-fit model – AIC of the corresponding null model). Sample-size corrected AIC values were used in all cases.

Data were analyzed using the R platform (R Core Team, 2018) and graphs were prepared using the ‘ggplot2’ package (Wickham, 2016). Robust t-tests were done by 10,000 bootstrapped samples considering mean as an estimator for group comparison, and implemented by the *pb2gen* function of the WRS2 R-package (Mair and Wilcox, 2018). Adjusted  $R^2$  values for GLMs were calculated using the *rsq* function of the R-package ‘rsq’ (Zhang, 2018).

## 235 **3 Results**

### **3.1 Seasonal albedo in post-harvest and post-fire stands**

Albedo differences between post-harvest and post-fire stands varied among seasons. Albedo values in periods of the year with appreciable snow cover were significantly higher in post-harvest stands than in post-fire stands (for winter: 0.56 vs. 0.34,  $p < 0.01$ ; for spring: 0.32 vs. 0.24,  $p = 0.11$ ). Summer albedo values were also marginally higher in post-harvest stands (240  $p = 0.24$ ), and fall albedos were similar between disturbance types ( $p = 0.73$ ) (Fig. 2). Considering stand age as a covariate, ANCOVA results also indicate higher albedo of post-harvest stands in winter ( $p = 0.02$ ), spring ( $p = 0.15$ ), summer ( $p = 0.04$ ), and similar in fall ( $p = 0.77$ ) compared to post-fire stands. Data also suggest higher variability in albedo in post-harvest stands than in post-fire stands (Fig. 2).

### **3.2 Ground surface reflectance in post-harvest and post-fire stands**

245 Specular-included reflectance measurements of ground surface samples suggest that differences in ground surface characteristics contribute to overall surface albedo in the study sites. Summer ground surface reflectance was generally higher in old stands (Fig. 3b) than in young stands (Fig. 3a) particularly in the 600–1000 nm range. Young (4-year old) post-harvest stands showed significantly lower mean ground reflectance values (74.3 %,  $p < 0.01$ ) in the visual spectrum (400–700 nm) and higher (32.3 %,  $p < 0.01$ ) in the near-infrared spectrum ( $> 700$ –1000 nm) than those of young post-fire stands (Fig. 3a). Older (11- and 19-year old) post-harvest stands however showed higher mean ground reflectance in both 250 visible (31.7%,  $p < 0.01$ ) and near-infrared (4.6%,  $p < 0.01$ ) spectra compared to post-fire stands (Fig. 3b).

### **3.3 Seasonal albedo in relation to stand attributes in post-harvest and post-fire stands**

#### **3.3.1 Winter albedo in post-harvest and post-fire stands**

255 Results from the best-fit GLM ( $p < 0.01$ , adj.  $R^2 = 0.97$ ) for post-harvest stands indicated that stand age, proportion of deciduous broadleaf species, canopy height, and interactions among these variables were significant predictors of winter albedo (Table 2). Stand age was related to winter albedo via an exponential decay model with a horizontal asymptote ( $\Delta AIC = -25.5$ ), and all estimated model parameters were significant (for 0.19 and 0.55:  $p < 0.01$ ; for  $-0.06$ :  $p < 0.05$ ) (Fig. 4a). The proportion of deciduous broadleaf species (Fig. 6a) and canopy height (Fig. 7a) were also related to winter 260 albedo via negative exponential models with horizontal asymptotes ( $\Delta AIC = -6.7$  and  $-100.4$ , respectively), and all estimated parameters for both models were significant ( $p < 0.01$ ).

For post-fire stands the best-fit GLM ( $p < 0.01$ , adj.  $R^2 = 0.75$ ) indicated that stand age and proportion of deciduous broadleaf species were significant predictors of winter albedo (Table 2). Stand age was related to winter albedo via an

265 exponential decay model with a horizontal asymptote ( $\Delta AIC = -38.5$ ), and all estimated model parameters were significant ( $p < 0.01$ ) (Fig. 4b). Proportion of deciduous broadleaf species was related to winter albedo via a negative exponential model with horizontal asymptote ( $\Delta AIC = -16.3$ ), and all estimated model parameters were significant (for  $-0.27$ :  $p < 0.06$ ; for  $1.02$  and  $0.45$ :  $p < 0.01$ ) (Fig. 6b).

### 270 **3.3.2 Spring albedo in post-harvest and post-fire stands**

For post-harvest stands the best-fit GLM ( $p < 0.01$ , adj.  $R^2 = 0.99$ ) indicated that stand age, proportion of deciduous broadleaf species, height, and the interaction of stand age and proportion of deciduous broadleaf species were significant predictors of spring albedo (Table 2). Stand age (Fig. 5a) and canopy height (Fig. 7c) were related to spring albedo via exponential decay models with horizontal asymptotes ( $\Delta AIC = -15.1$  and  $-31.2$ , respectively). Estimated parameters of stand age-albedo (for  $0.26$ :  $p < 0.01$ ; for  $0.72$  and  $-0.72$ :  $p < 0.05$ ) and canopy height-albedo (for  $0.16$  and  $0.33$ :  $p < 0.01$ ; for  $-1.84$ :  $p = 0.07$ ) models were likewise significant. The proportion of deciduous broadleaf species was related to spring albedo via a negative exponential model ( $\Delta AIC = -6.72$ ), and all estimated parameters were significant ( $p < 0.01$ ) (Fig. 6c).

The best-fit GLM ( $p < 0.01$ , adj.  $R^2 = 0.99$ ) for post-fire stands indicated that stand age and proportion of deciduous broadleaf species were the only significant predictors of spring albedo (Table 2). Stand age (Fig. 5b) and proportion of deciduous broadleaf species (Fig. 6d) were related to spring post-fire stand albedo via exponential negative growth models ( $\Delta AIC = -7.0$  and  $-7.5$ , respectively), and all estimated parameters for both models were significant ( $p < 0.01$ ).

### **3.3.3 Summer albedo in post-harvest and post-fire stands**

285 The best-fit GLM ( $p < 0.01$ , adj.  $R^2 = 0.97$ ) for post-harvest stands indicated that stand age, proportion of deciduous broadleaf species, ground vegetation cover and its interaction with stand age and proportion of deciduous broadleaf species were significant predictors of summer albedo (Table 2). Stand age was related to summer albedo via a double exponential model ( $\Delta AIC = -73.1$ ), and all estimated model parameters were significant ( $p < 0.01$ ) (Fig. 4c). The pattern described by this function indicates a sharp peak in albedo with a maximum at 10–15 years of stand age. Proportion of deciduous broadleaf species is related to summer albedo via a 3-parameter sigmoid model ( $\Delta AIC = -48.6$ ), and all the estimated parameters were significant ( $p < 0.01$ ) (Fig. 6e). Ground vegetation cover was related to summer albedo via an exponential model with a Gumbel distribution without a horizontal asymptote ( $\Delta AIC = -25.8$ ), and all estimated parameters were significant ( $p < 0.01$ ) (Fig. 8e).

295 For post-fire stands the best-fit GLM ( $p < 0.01$ , adj.  $R^2 = 0.95$ ) indicated that stand age, proportion of deciduous broadleaf species, canopy height, and their interactions with stand age were significant predictors of summer albedo (Table 2). Stand age (Fig. 4d) and canopy height (Fig. 7f) were related to summer post-fire stand albedo via exponential models with Gumbel distributions with horizontal asymptotes ( $\Delta AIC = -49.3$  and  $-5.3$ , respectively). As in the case of post-harvest stands, peak albedo was found at  $\sim 10$ – $15$  years of stand age. All estimated parameters of stand age-albedo and canopy height-albedo models were significant ( $p < 0.01$ ). Proportion of deciduous broadleaf species was related to summer albedo via a negative exponential growth model ( $\Delta AIC = -6.8$ ), and all estimated model parameters were significant ( $p < 0.01$ ) (Fig. 6f).



### 3.3.4 Fall albedo in post-harvest and post-fire stands

305 The best-fit GLM ( $p < 0.01$ , adj.  $R^2 = 0.94$ ) for post-harvest stands indicated that stand age, canopy height, ground  
vegetation cover, and their interactions were significant predictors of fall albedo (Table 2). Proportion of deciduous  
broadleaf species was also an important predictor that was modelled separately via a double exponential model (and was not  
added to the GLM to avoid modelling complexities) ( $\Delta AIC = -0.9$ ); all estimated model parameters were significant (for  
28.9 and 45.4:  $p < 0.05$ ; for 67.6:  $p < 0.01$ ) (Fig. 6g). Stand age (Fig. 5c) and ground vegetation cover (Fig. 8g) were related  
310 to albedo via exponential decay models with horizontal asymptotes ( $\Delta AIC = -36.8$  and  $-28.38$ , respectively), and all  
estimated parameters for both models were significant ( $p < 0.01$ ). Canopy height was also related to albedo via a negative  
exponential model ( $\Delta AIC = -11.2$ ), and all estimated parameters were significant ( $p < 0.01$ ) (Fig. 7g).

To avoid modelling complexities, stand age and proportion of deciduous broadleaf species were fitted individually with fall  
315 albedo of post-fire stands (Table 2). Stand age was related to albedo via a double exponential model ( $\Delta AIC = -3.1$ ), and all  
estimated model parameters were significant ( $p < 0.01$ ) (Fig. 5d). Proportion of deciduous broadleaf species was generally  
related to albedo via a simple exponential model ( $\Delta AIC = -25.4$ ), and all estimated model parameters were significant ( $p <$   
0.01) (Fig. 6h). In the case of fall albedo in post-harvest stands, there is an apparent decline in nearly pure stands (Fig. 6g),  
with a better fit of the double exponential model. We speculate that very dark post-senescence leaf litter of aspen may  
320 account for this effect.

## 4 Discussion

Our results provide evidence for dramatic effects of disturbance type on the albedo of boreal forest systems, with post-  
harvest stands showing much higher albedo values in winter and spring months than post-fire stands. Stands of both  
disturbance types also showed strongly age-dependent patterns in albedo; however, analyses suggest that post-disturbance  
325 changes are more gradual than anticipated, with dynamics continuing past stand closure, up to  $\sim 50$  years post-disturbance.  
The proportion of deciduous species also had large effects on stand albedo – generally larger than stand age effects –  
showing a positive saturating response in all seasons and for both disturbance types.

### 4.1 Albedo in post-harvest and post-fire stands

330 Mean albedo in post-harvest stands was significantly higher than in post-fire stands in winter and spring, marginally higher  
in summer, and similar in fall (Fig. 2). A similar pattern in albedo differences was also observed when the stand age effects  
on albedo were statistically controlled. The magnitude of differences in winter and spring values (0.22 and 0.08, or 63% and  
34% increases relative to post-fire values) is large – comparable to albedo differences observed between biomes (Stephens  
et al., 2015). During snow-covered seasons (winter and spring), charcoal residues in post-fire stands are usually covered  
335 with snow, and thus stand structure and composition act as dominant drivers of albedo (Lyons et al., 2008; Amiro et al.,  
2006b; Liu et al., 2005). Deciduous broadleaf species made up 37.8 % of basal area in post-fire stands and 55.4 % in post-  
harvest stands: the higher percentage of dark conifer leaves is expected to result in lower winter/spring albedos in post-fire  
stands compared to post-harvest stands (Betts and Ball, 1997). However, immediately after a stand-replacing fire, the  
presence of black carbon (charcoal and soot) in the snow can reduce early winter albedo and possibly enhance spring  
340 snowmelt by absorbing solar radiation (Qian et al., 2009; Conway et al., 1996). During late spring when snow cover is  
shallow, it is also likely that charred branches and stems protrude through the snow and reduce albedo. From an energy

balance perspective, it is important to note that albedo differences in late spring may be less important as turbulent and latent fluxes likely dominate (Conway et al., 1996).

345 In snow-free seasons (summer and fall) the marginal differences in mean albedo between post-harvest and post-fire stands can partly be attributed to rapid recovery of ground vegetation in post-fire stands (0–5 years old) compared to post-harvest stands (Bartels et al., 2016), and to the vegetation covering dark charcoals in older (> 5 year) post-fire stands (Randerson et al., 2006). Soon after a fire, the presence of early-successional plants (Johnstone et al., 2010) can increase surface albedo of post-fire stands because of their higher albedo relative to charcoal (Amiro et al., 2006b; Betts and Ball, 1997). This effect is  
350 expected to offset the albedo difference between post-harvest and post-fire stands. In the first year following disturbance events, we might expect lower snow-free albedo in post-fire stands than post-harvest stands because of high charcoal occurrence on the soil surface (Lyons et al., 2008; Chambers and Chapin, 2002). However, our soil reflectance data indicate that soils from 4-year old post-fire stands unexpectedly showed significantly higher reflectance in the visible spectrum than did post-harvest stands (with the pattern reversed in the NIR spectrum) (Fig. 3a). Similar patterns in spectral response were  
355 recently observed in a biochar-amended agricultural soil relative to the control (Zhang et al., 2013). Soils from older post-harvest stands (11- and 19-year old), as expected, showed higher reflectance in the visible and NIR spectra compared to post-fire stands of similar age (Fig. 3b). Most post-harvest stands exhibited patches of charcoal in surface soils, presumably originating from historical fires (personal observations). The importance of “legacy” soil charcoal on surface albedo of harvested stands has not been considered previously to our knowledge. Charcoal reflectance is highly dependent on charring  
360 conditions (e.g., temperature, oxygen content) (Hudspith et al., 2015), and may possibly change with weathering; these processes require additional study in the context of albedo and surface energy balance.

Our results from both snow-covered and snow-free seasons strongly suggest that fire residues on the ground cannot explain the observed differences in albedo between post-harvest and post-fire stands. This result is consistent with the generalization  
365 that stand structure and composition are the main drivers of surface albedo and energy balance in the boreal forest (Amiro et al., 2006a).

#### **4.2 Albedo convergence with stand age in post-harvest and post-fire stands**

Compiled data for winter and summer albedos from post-harvest and post-fire stands indicate that surface albedo saturates  
370 at ~ 50 years of stand age in the boreal forest (Figs. 4a–d). This finding does not support our second hypothesis that albedo saturates after ~ 25 years of stand age (during the ‘stem exclusion’ phase). The rationale behind this hypothesis was that a high cover of deciduous species until ~ 25 years contributes to high albedo in both snow-covered (due to leaf shedding) and snow-free (due to high canopy albedo) seasons; after this age, deciduous species are replaced by conifers and albedo tends to saturate (Kuusinen et al., 2014; Amiro et al., 2006b). Studies using remote sensing techniques also suggest that albedo in  
375 both post-harvest and post-fire stands saturates at ~ 50 years after harvest/fire (Bright et al., 2015a; Kuusinen et al., 2014; Lyons et al., 2008; McMillan and Goulden, 2008), consistent with our findings. These results thus suggest that gradual changes in species composition through later stages of succession are an important driver of stand albedo. Stand structural features such as canopy height (in winter) and ground vegetation cover (in summer) usually increase with stand age (Bartels et al., 2016) and might additionally contribute to a gradual reduction in albedo (Hovi et al., 2016) after ~ 25 years (Table 2,  
380 Figs. 7 and 8).

The shape of best-fit curves for winter albedo vs. stand age (exponential decay) of post-harvest (Fig. 4a) and post-fire (Fig. 4b) stands are similar to other studies (Bright et al., 2015b; Kuusinen et al., 2014; Lyons et al., 2008; McMillan and Goulden, 2008; Amiro et al., 2006b); however our results diverge markedly for summer albedo. Our best-fit curves for summer albedo vs. stand age for both post-harvest and post-fire stands showed pronounced peaks in early albedo described by double exponential functions (Fig. 4c–d), whereas Amiro et al (2006b) described data with a negative linear relationship, and other remote sensing-based studies have used exponential decay curves (e.g., Kuusinen et al., 2014). However, Lyons et al. (2008) and Randerson et al. (2006) found summer albedo of post-fire stands were related to stand age via a humped-shape curve, and albedo reached peak at ~ 20 years and gradually levelled off at ~ 50 years after fire, which closely corresponds to our findings (although our observed peak is at ~10 years post-disturbance: Fig. 4c–d). We suggest that most prior studies with sparser or more noisy data sets may have missed this early peak pattern. Immediately after fires and harvesting (because of high soil moisture, decaying CWD, legacy charcoal etc.) the summer albedo of post-harvest and post-fire stands is expected to show a low value (also see section 4.1 and Fig. 3) which sharply increases as dark ground is covered with early successional pioneer species (Lyons et al., 2008; Randerson et al., 2006; Amiro et al., 2006b; Betts and Ball, 1997). This sharp increase continues until ~ 20 years of stand age but then decreases slowly until ~ 50 years and saturates – consistent with the patterns found in other seasons.

We did not have albedo data from late-seral post-harvest or post-fire stands for spring and fall. In post-harvest (Fig. 5a) and post-fire (Fig. 5b) stands spring albedos did not show strong patterns with stand age, and the patterns were disturbance-specific (exponential decrease vs. negative exponential growth, respectively). Results from Kuusinen et al. (2014), Lyons et al. (2008), and Randerson et al. (2006) also suggest that patterns of spring albedo as a function of stand age can be disturbance-specific. In post-harvest stands, Kuusinen et al. (2014) found that spring albedo was high immediately after harvest and decreased exponentially until ~ 50 years and then saturated. However, in post-fire stands, Lyons et al. (2008) and Randerson et al. (2006), found hump-shaped patterns with a peak at ~ 10–15 years, and subsequent declines, similar to the winter albedo pattern. As discussed in Section 4.1, disturbance-specific responses may partially be attributed to the presence of black carbon (charcoal/soot) in snow immediately after a fire, which can substantially reduce snow albedo (Qian et al., 2009). Trends in fall albedo values with stand age in post-harvest (Fig. 5c) and post-fire (Fig. 5d) stands showed stronger patterns than spring, but similar disturbance-specific responses. Immediately after harvesting fall albedo was high, and exponentially decreased as stand age increased. Increased fall albedo in recent post-harvest stands may be due to contributions to senescing leaves and to snow in the late fall (Amiro et al., 2006b; Liu et al., 2005). In contrast, fall albedo immediately after a fire was low (possibly because of charcoal or soot residues as discussed above), and increased with stand age.

Predicting albedo has been a classical problem in climate simulations (Bright et al., 2015a; Kuusinen et al., 2012; Qu and Hall, 2007). Our findings indicate that there are important qualitative differences in the post-disturbance albedo patterns between seasons in boreal forests. These differences need to be considered in enhancing albedo predictability of land surface models.

### 4.3 Deciduous broadleaf species as a key determinant of surface albedo in the post-harvest and post-fire stands

420 Our results indicate that the proportion of deciduous broadleaf species is a strong predictor of albedo irrespective of disturbance type, and in most cases a better predictor than stand age (Figs. 4–6). Using remote sensing techniques Kuusinen et al. (2014) also found that stand age alone was not consistently the best predictor of stand albedo in the boreal forest. We found a similar mean model residual sum of errors for snow-covered seasons and snow-free seasons (Figs. 4–5 vs. Fig. 6), indicating that the proportion of deciduous broadleaf species are similarly important in both cases. These findings strongly support our third hypothesis that stands with a higher proportion of deciduous broadleaf species show higher albedo than conifer-dominated stands, but also that this effect is pronounced under both snow-covered and snow-free conditions. Except for fall post-fire stands, the relationship between albedo and proportion of deciduous broadleaf species approximated by an exponential saturating curve in which albedo declined rapidly where the proportion of deciduous broadleaf species fell below 25–50 %. Fall albedo in post-fire stands, on the other hand, was found to be even more sensitive, with a drop in fall albedo at a proportion of deciduous broadleaf species below 80%. We speculate that this sensitivity was related to exposure of fire residues in early stand development.

Overall our results indicate a strong dependency of seasonal albedo on the proportion of deciduous broadleaf species both in post-harvest and post-fire stands. This effect provides a strong link between albedo and successional patterns in mixedwood boreal forests. Prior studies addressing this relationship (e.g., Lyons et al., 2008; Amiro et al., 2006b) have suggested that increasing deciduous tree cover results in increased albedo values from stand initiation to ~ 25 years of stand age; thereafter, conifers start dominating the canopy, canopy height increases, and albedo decreases gradually until ~ 50 years of stand age before reaching a steady state. The data presented in the current study provide a somewhat different picture of these trends, in that patterns show important quantitative differences depending on the season and disturbance type. The importance of deciduous broadleaf species in the albedo signal over ~ 50 years of stand development suggests that slow successional changes in species composition are likely the main driver of the age-related patterns in mixedwood boreal forests albedo. The dynamics of this pattern is likely to depend on the intensity and frequency of disturbance, edaphic conditions, species abundance, and climate (Taylor and Chen, 2011). For example, in dry nutrient-poor boreal stands, deciduous broadleaf species-driven albedo might never occur, as such stands are commonly dominated by jack pine (Taylor and Chen, 2011); however, in mesic moderate-nutrient-rich stands, deciduous broadleaf species can dominate for ~ 100 years (Cogbill, 1985). Future studies should prioritize robust modelling of boreal succession pathways under different biotic/abiotic conditions to properly characterize stand albedo.

## 5 Conclusions

Our findings have important implications for climate-friendly forest management practices. Since the proportion of deciduous broadleaf species is a strong predictor of seasonal albedo, stand-level albedo can be increased by enhancing the proportion of deciduous broadleaf species in a stand. Precisely this approach has recently been suggested as an adaptation and mitigation strategy to counter negative climate forcings of boreal forest (Astrup et al., 2018), but empirical data from actual managed stands have been lacking. Historically, forest managers have commonly sought to decrease or eliminate deciduous species and enhance conifers. However, there is strong evidence that local tree diversity enhances productivity in boreal forests as in other systems (Paquette and Messier, 2011), and in particular that mixedwood boreal forests including both conifers and deciduous trees show high productivity (MacPherson et al., 2001; Zhang et al., 2012). Management to

increase the proportion of deciduous broadleaf species in managed boreal forests (for example, simply by avoiding chemical herbicide used to kill deciduous broadleaf species or retaining deciduous broadleaf species seed-trees) could thus be a “win-win” scenario for enhanced carbon sequestration via primary productivity, and climate mitigation via enhanced albedo.

460

In climate modeling studies albedo estimation for boreal forests have commonly been achieved by highly simplified representations of vegetation dynamics (Thackeray et al., 2019). In a recent study, Bright et al. (2018) pointed out that overlooking stand structural and compositional properties over the successional trajectory is likely to substantially bias radiative forcing estimates in the boreal forest. Ground-based estimates such as those presented are essential: at high latitudes when solar zenith angle is high ( $> 70^\circ$ ), satellites such as MODIS often provide poor-quality albedo data due to spatial heterogeneity of the landscape pixel signature and performance degradation of atmospheric correction algorithms (Bright et al., 2015b; Wang et al., 2012). Our findings based on field data are thus important in evaluating and potentially improving albedo predictions in land surface characterizations with climate models, and in improving albedo estimates derived from remote sensing. In addition, our results point to the importance of slow ecological succession as a driver of age-related patterns in albedo, suggesting that future models should explicitly incorporate these ecological processes to better predict long-term trends in climate forcings in boreal forests.

465

470

## **6 Code availability**

R (version 3.5.1) codes used in the data analysis can be requested to M.A.H. ([abdul.halim@mail.utoronto.ca](mailto:abdul.halim@mail.utoronto.ca)).

## **7 Data availability**

475

Data used to produce the graphs are also available via requesting corresponding author ([abdul.halim@mail.utoronto.ca](mailto:abdul.halim@mail.utoronto.ca)).

## **8 Author contribution**

M.A.H., H.Y.H.C., and S.C.T. designed the experiment. M.A.H. analysed data with inputs from S.C.T. and H.Y.H.C. M.A.H. wrote the manuscript with edits and comments from H.Y.H.C. and S.C.T.

## **9 Competing interests**

480

The authors declare no competing interests.

## **10 Acknowledgements**

Authors acknowledge assistances from Jillian Bieser, Kyle Gaynor, Lutchmee Sujeeun, Jack Richard, Jad Murtada, Anna Almero, and Hiro Sato during experiment setup and data collection. We thank Mark Horsburgh for his helpful comments on an earlier version of this manuscript and Shannon Brown for her help during the field comparison of pyranometers. We would also like to thank two anonymous reviewers and the editor for their critical comments, which helped to improve the manuscript. This study was funded by the NSERC (Natural Sciences and Engineering Research Council of Canada) Strategic Grant (grant number: STPGP 428641) and the NSERC Discovery Grant (grant number: RGPIN 06209).

485

## 11 References

- 490 Amiro, B., Barr, A., Black, T., Iwashita, H., Kljun, N., Mccaughey, J., Morgenstern, K., Murayama, S., Nestic, Z. and Orchansky, A.: Carbon, energy and water fluxes at mature and disturbed forest sites, Saskatchewan, Canada, *Agric. For. Meteorol.*, 136(3–4), 237–251, doi:10.1016/j.agrformet.2004.11.012, 2006a.
- Amiro, B. D., Orchansky, A. L., Barr, A. G., Black, T. A., Chambers, S. D., Chapin III, F. S., Goulden, M. L., Litvak, M., Liu, H. P., Mccaughey, J. H., McMillan, A. and Randerson, J. T.: The effect of post-fire stand age on the boreal forest energy balance, *Agric. For. Meteorol.*, 140(1), 41–50, doi:10.1016/j.agrformet.2006.02.014, 2006b.
- 495 Astrup, R., Bernier, P. Y., Genet, H., Lutz, D. A. and Bright, R. M.: A sensible climate solution for the boreal forest, *Nat. Clim. Change*, 8(1), 11–12, doi:10.1038/s41558-017-0043-3, 2018.
- Bala, G., Caldeira, K., Wickett, M., Phillips, T. J., Lobell, D. B., Delire, C. and Mirin, A.: Combined climate and carbon-cycle effects of large-scale deforestation, *Proc. Natl. Acad. Sci.*, 104(16), 6550–6555, doi:10.1073/pnas.0608998104, 2007.
- 500 Baltzer, J. L. and Thomas, S. C.: Leaf optical responses to light and soil nutrient availability in temperate deciduous trees, *Am. J. Bot.*, 92(2), 214–223, 2005.
- Bartels, S. F., Chen, H. Y. H., Wulder, M. A. and White, J. C.: Trends in post-disturbance recovery rates of Canada’s forests following wildfire and harvest, *For. Ecol. Manag.*, 361, 194–207, doi:10.1016/j.foreco.2015.11.015, 2016.
- Betts, A. K. and Ball, J. H.: Albedo over the boreal forest, *J. Geophys. Res. Atmospheres*, 102(D24), 28901–28909, doi:10.1029/96JD03876, 1997.
- 505 Betts, R. A.: Offset of the potential carbon sink from boreal forestation by decreases in surface albedo, *Nature*, 408(6809), 187–190, doi:10.1038/35041545, 2000.
- Brassard, B. W. and Chen, H. Y. H.: Effects of Forest Type and Disturbance on Diversity of Coarse Woody Debris in Boreal Forest, *Ecosystems*, 11(7), 1078–1090, doi:10.1007/s10021-008-9180-x, 2008.
- Brassard, B. W. and Chen, H. Y. H.: Stand Structure and Composition Dynamics of Boreal Mixedwood Forest: Implications for Forest Management, *Sustainable Forest Management Network.*, 2010.
- 510 Brassard, B. W., Chen, H. Y. H., Wang, J. R. and Duinker, P. N.: Effects of time since stand-replacing fire and overstory composition on live-tree structural diversity in the boreal forest of central Canada, *Can. J. For. Res.*, 38(1), 52–62, doi:10.1139/X07-125, 2008.
- Bright, R. M., Astrup, R. and Strømman, A. H.: Empirical models of monthly and annual albedo in managed boreal forests of interior Norway, *Clim. Change*, 120(1–2), 183–196, doi:10.1007/s10584-013-0789-1, 2013.
- 515 Bright, R. M., Zhao, K., Jackson, R. B. and Cherubini, F.: Quantifying surface albedo and other direct biogeophysical climate forcings of forestry activities, *Glob. Change Biol.*, 21(9), 3246–3266, doi:10.1111/gcb.12951, 2015a.
- Bright, R. M., Myhre, G., Astrup, R., Antón-Fernández, C. and Strømman, A. H.: Radiative forcing bias of simulated surface albedo modifications linked to forest cover changes at northern latitudes, *Biogeosciences*, 12(7), 2195–2205, doi:10.5194/bg-12-2195-2015, 2015b.
- 520 Bright, R. M., Eisner, S., Lund, M. T., Majasalmi, T., Myhre, G. and Astrup, R.: Inferring Surface Albedo Prediction Error Linked to Forest Structure at High Latitudes, *J. Geophys. Res. Atmospheres*, 123(10), 4910–4925, doi:10.1029/2018JD028293, 2018.
- Brown, P. T. and Caldeira, K.: Greater future global warming inferred from Earth’s recent energy budget, *Nature*, 552(7683), 45–50, doi:10.1038/nature24672, 2017.
- 525 Chambers, S. D. and Chapin, F. S.: Fire effects on surface-atmosphere energy exchange in Alaskan black spruce ecosystems: Implications for feedbacks to regional climate, *J. Geophys. Res.*, 108(D1), doi:10.1029/2001JD000530, 2002.

- Chen, H. Y. and Popadiouk, R. V.: Dynamics of North American boreal mixedwoods, *Environ. Rev.*, 10(3), 137–166, doi:10.1139/a02-007, 2002.
- 530 Chen, H. Y. H., Vasiliauskas, S., Kayahara, G. J. and Ilsson, T.: Wildfire promotes broadleaves and species mixture in boreal forest, *For. Ecol. Manag.*, 257(1), 343–350, doi:10.1016/j.foreco.2008.09.022, 2009.
- Cogbill, C. V.: Dynamics of the boreal forests of the Laurentian Highlands, Canada, *Can. J. For. Res.*, 15(1), 252–261, doi:10.1139/x85-043, 1985.
- Colombo, S. J., Parker, W. C., Luckai, N., Dang, Q. and Cai, T.: The Effects of Forest Management on Carbon Storage in Ontario's Forests, Climate Change Research Report, Ontario Forest Research Institute, Ministry of Natural Resources, Canada, Toronto: Queens Printer for Ontario. [online] Available from: [http://www.climateontario.ca/MNR\\_Publications/276922.pdf](http://www.climateontario.ca/MNR_Publications/276922.pdf), 2005.
- 535
- Conway, H., Gades, A. and Raymond, C. F.: Albedo of dirty snow during conditions of melt, *Water Resour. Res.*, 32(6), 1713–1718, doi:10.1029/96WR00712, 1996.
- 540 Environment Canada: Historical climate data, [online] Available from: [http://climate.weather.gc.ca/historical\\_data/search\\_historic\\_data\\_e.html](http://climate.weather.gc.ca/historical_data/search_historic_data_e.html) (Accessed 11 January 2018), 2018.
- Halim, M. A. and Thomas, S. C.: Surface albedo in relation to disturbance and early stand dynamics in the boreal forest: Implications for climate models., p. abstract #B21F-2025, American Geophysical Union Fall Meeting, 11-15 December 2017, New Orleans, USA., 2017.
- 545 Halim, M. A. and Thomas, S. C.: A proxy-year analysis shows reduced soil temperatures with climate warming in boreal forest, *Sci. Rep.*, 8(1), doi:10.1038/s41598-018-35213-w, 2018.
- Hansen, J., Sato, M., Ruedy, R., Nazarenko, L., Lacis, A., Schmidt, G. A., Russell, G., Aleinov, I., Bauer, M., Bauer, S., Bell, N., Cairns, B., Canuto, V., Chandler, M., Cheng, Y., Del, G. A., Faluvegi, G., Fleming, E., Friend A., Hall T., Jackman C., Kelley M., Kiang N., Koch D., Lean J., Lerner J., Lo K., Menon S., Miller R., Minnis P., Novakov T., Oinas V., Perlwitz Ja., Perlwitz Ju., Rind D., Romanou A., Shindell D., Stone P., Sun S., Tausnev N., Thresher D., Wielicki B., Wong T., Yao M. and Zhang, S.: Efficacy of climate forcings, *J. Geophys. Res. Atmospheres*, 110(D18), doi:10.1029/2005JD005776, 2005.
- 550
- Hart, S. and Luckai, N.: Charcoal function and management in boreal ecosystems, edited by P. Brando, *J. Appl. Ecol.*, 1197–1206, doi:10.1111/1365-2664.12136, 2013.
- 555 Hovi, A., Liang, J., Korhonen, L., Kobayashi, H. and Rautiainen, M.: Quantifying the missing link between forest albedo and productivity in the boreal zone, *Biogeosciences*, 13(21), 6015–6030, doi:10.5194/bg-13-6015-2016, 2016.
- Hudspith, V. A., Belcher, C. M., Kelly, R. and Hu, F. S.: Charcoal Reflectance Reveals Early Holocene Boreal Deciduous Forests Burned at High Intensities, *PLoS ONE*, 10(4), doi:10.1371/journal.pone.0120835, 2015.
- 560 Johnstone, J. F., Hollingsworth, T. N., Chapin, F. S. and Mack, M. C.: Changes in fire regime break the legacy lock on successional trajectories in Alaskan boreal forest, *Glob. Change Biol.*, 16(4), 1281–1295, doi:10.1111/j.1365-2486.2009.02051.x, 2010.
- Kirschbaum, M. U. F., Whitehead, D., Dean, S. M., Beets, P. N., Shepherd, J. D. and Ausseil, A.-G. E.: Implications of albedo changes following afforestation on the benefits of forests as carbon sinks, *Biogeosciences*, 8(12), 3687–3696, doi:10.5194/bg-8-3687-2011, 2011.
- 565 Kumar, P., Chen, H. Y. H., Thomas, S. C. and Shahi, C.: Epixylic vegetation abundance, diversity, and composition vary with coarse woody debris decay class and substrate species in boreal forest, *Can. J. For. Res.*, 48(4), 399–411, doi:10.1139/cjfr-2017-0283, 2018.
- Kuusinen, N., Kolari, P., Levula, J., Porcar-Castell, A., Stenberg, P. and Berninger, F.: Seasonal variation in boreal pine forest albedo and effects of canopy snow on forest reflectance, *Agric. For. Meteorol.*, 164, 53–60, doi:10.1016/j.agrformet.2012.05.009, 2012.
- 570

- Kuusinen, N., Tomppo, E., Shuai, Y. and Berninger, F.: Effects of forest age on albedo in boreal forests estimated from MODIS and Landsat albedo retrievals, *Remote Sens. Environ.*, 145, 145–153, doi:10.1016/j.rse.2014.02.005, 2014.
- 575 Kuusinen, N., Stenberg, P., Tomppo, E., Bernier, P. and Berninger, F.: Variation in understory and canopy reflectance during stand development in Finnish coniferous forests, *Can. J. For. Res.*, 45(8), 1077–1085, doi:10.1139/cjfr-2014-0538, 2015.
- Kuusinen, N., Stenberg, P., Korhonen, L., Rautiainen, M. and Tomppo, E.: Structural factors driving boreal forest albedo in Finland, *Remote Sens. Environ.*, 175, 43–51, doi:10.1016/j.rse.2015.12.035, 2016.
- 580 Lee, X., Goulden, M. L., Hollinger, D. Y., Barr, A., Black, T. A., Bohrer, G., Bracho, R., Drake, B., Goldstein, A., Gu, L., Katul, G., Kolb, T., Law, B. E., Margolis, H., Meyers, T., Monson, R., Munger, W., Oren, R., Paw U, K. T., Richardson, A. D., Schmid, H. P., Staebler, R., Wofsy, S. and Zhao, L.: Observed increase in local cooling effect of deforestation at higher latitudes, *Nature*, 479(7373), 384–387, doi:10.1038/nature10588, 2011.
- Li, Y., Wang, T., Zeng, Z., Peng, S., Lian, X. and Piao, S.: Evaluating biases in simulated land surface albedo from CMIP5 global climate models: Albedo Evaluation in CMIP5, *J. Geophys. Res. Atmospheres*, 121(11), 6178–6190, doi:10.1002/2016JD024774, 2016.
- 585 Linacre, E.: *Climate Data and Resources: A Reference and Guide*, e-book., Routledge, London., 2003.
- Liu, H., Randerson, J. T., Lindfors, J. and Chapin, F. S.: Changes in the surface energy budget after fire in boreal ecosystems of interior Alaska: An annual perspective, *J. Geophys. Res.*, 110(D13), doi:10.1029/2004JD005158, 2005.
- Lukeš, P., Stenberg, P., Rautiainen, M., Mõttus, M. and Vanhatalo, K. M.: Optical properties of leaves and needles for boreal tree species in Europe, *Remote Sens. Lett.*, 4(7), 667–676, doi:10.1080/2150704X.2013.782112, 2013a.
- 590 Lukeš, P., Stenberg, P. and Rautiainen, M.: Relationship between forest density and albedo in the boreal zone, *Ecol. Model.*, 261–262, 74–79, doi:10.1016/j.ecolmodel.2013.04.009, 2013b.
- Luyssaert, S., Marie, G., Valade, A., Chen, Y.-Y., Njakou Djomo, S., Ryder, J., Otto, J., Naudts, K., Lansø, A. S., Ghattas, J. and McGrath, M. J.: Trade-offs in using European forests to meet climate objectives, *Nature*, 562(7726), 259–262, doi:10.1038/s41586-018-0577-1, 2018.
- 595 Lyons, E. A., Jin, Y. and Randerson, J. T.: Changes in surface albedo after fire in boreal forest ecosystems of interior Alaska assessed using MODIS satellite observations, *J. Geophys. Res. Biogeosciences*, 113(G02012), doi:10.1029/2007JG000606, 2008.
- MacPherson, D. M., Lieffers, V. J. and Blenis, P. V.: Productivity of aspen stands with and without a spruce understory in Alberta's boreal mixedwood forests, *For. Chron.*, 77(2), 351–356, doi:10.5558/tfc77351-2, 2001.
- 600 Madoui, A., Gauthier, S., Leduc, A., Bergeron, Y. and Valeria, O.: Monitoring Forest Recovery Following Wildfire and Harvest in Boreal Forests Using Satellite Imagery, *Forests*, 6(12), 4105–4134, doi:10.3390/f6114105, 2015.
- Mair, P. and Wilcox, R.: WRS2: Wilcox robust estimation and testing, R package. [online] Available from: <https://r-forge.r-project.org/projects/psychor/>, 2018.
- 605 Matthies, B. D. and Valsta, L. T.: Optimal forest species mixture with carbon storage and albedo effect for climate change mitigation, *Ecol. Econ.*, 123, 95–105, doi:10.1016/j.ecolecon.2016.01.004, 2016.
- McMillan, A. M. S. and Goulden, M. L.: Age-dependent variation in the biophysical properties of boreal forests: Biophysical Properties of boreal forests, *Glob. Biogeochem. Cycles*, 22(2), n/a-n/a, doi:10.1029/2007GB003038, 2008.
- 610 Moussaoui, L., Fenton, N., Leduc, A. and Bergeron, Y.: Can Retention Harvest Maintain Natural Structural Complexity? A Comparison of Post-Harvest and Post-Fire Residual Patches in Boreal Forest, *Forests*, 7(12), 243, doi:10.3390/f7100243, 2016.



- Myers, D. R.: Comparison of direct normal irradiance derived from silicon and thermopile global hemispherical radiation detectors, edited by N. G. Dhere, J. H. Wohlgenuth, and K. Lynn, p. 77730G, San Diego, California., 2010.
- Naudts, K., Chen, Y., McGrath, M. J., Ryder, J., Valade, A., Otto, J. and Luyssaert, S.: Europes forest management did not mitigate climate warming, *Science*, 351(6273), 597–600, doi:10.1126/science.aad7270, 2016.
- 615 OMNRF: Forest Management Guide to Silviculture in the Great Lakes-St. Lawrence and Boreal Forests of Ontario., Ontario Legislative Library (OGDC) Open Access Electronic Government Documents, Ministry of Natural Resources and Forestry, Toronto: Queens Printer for Ontario. [online] Available from: <https://docs.ontario.ca/documents/4125/revised-silvguide-mar-2015-aoda-compliant.pdf>, 2015.
- 620 Paquette, A. and Messier, C.: The effect of biodiversity on tree productivity: from temperate to boreal forests: The effect of biodiversity on the productivity, *Glob. Ecol. Biogeogr.*, 20(1), 170–180, doi:10.1111/j.1466-8238.2010.00592.x, 2011.
- Qian, Y., Gustafson, W. I., Leung, L. R. and Ghan, S. J.: Effects of soot-induced snow albedo change on snowpack and hydrological cycle in western United States based on Weather Research and Forecasting chemistry and regional climate simulations, *J. Geophys. Res.*, 114(D3), doi:10.1029/2008JD011039, 2009.
- 625 Qu, X. and Hall, A.: What controls the strength of snow-albedo feedback?, *J. Clim.*, 20(15), 3971–3981, doi:10.1175/JCLI4186.1, 2007.
- R Core Team: R: A language and environment for statistical computing., R Foundation for Statistical Computing, Vienna, Austria. [online] Available from: URL <https://www.R-project.org/>, 2018.
- 630 Randerson, J. T., Liu, H., Flanner, M. G., Chambers, S. D., Jin, Y., Hess, P. G., Pfister, G., Mack, M. C., Treseder, K. K., Welp, L. R., Chapin, F. S., Harden, J. W., Goulden, M. L., Lyons, E., Neff, J. C., Schuur, E. A. G. and Zender, C. S.: The Impact of Boreal Forest Fire on Climate Warming, *Science*, 314(5802), 1130–1132, doi:10.1126/science.1132075, 2006.
- Rohatgi, A.: WebPlotDigitizer, Austin, Texas, USA. [online] Available from: <https://automeris.io/WebPlotDigitizer>, 2018.
- Sims, R. A., Towill, W. D., Baldwin, K. A. and Wickware, G. M.: Field guide to the forest ecosystem classification for northwestern Ontario., 2nd ed., Ontario Ministry of Natural Resources, Northwest Science and Technology, Thunder Bay, Ontario., 1997.
- 635 Stephens, G. L., O'Brien, D., Webster, P. J., Pilewski, P., Kato, S. and Li, J.: The albedo of Earth, *Rev. Geophys.*, 53(1), 141–163, doi:10.1002/2014RG000449, 2015.
- Stroeve, J., Box, J. E., Gao, F., Liang, S., Nolin, A. and Schaaf, C.: Accuracy assessment of the MODIS 16-day albedo product for snow: comparisons with Greenland in situ measurements, *Remote Sens. Environ.*, 94(1), 46–60, doi:10.1016/j.rse.2004.09.001, 2005.
- 640 Taylor, A. R. and Chen, H. Y. H.: Multiple successional pathways of boreal forest stands in central Canada, *Ecography*, 34(2), 208–219, doi:10.1111/j.1600-0587.2010.06455.x, 2011.
- Thackeray, C. W., Fletcher, C. G. and Derksen, C.: Diagnosing the Impacts of Northern Hemisphere Surface Albedo Biases on Simulated Climate, *J. Clim.*, 32(6), 1777–1795, doi:10.1175/JCLI-D-18-0083.1, 2019.
- 645 Uotila, A. and Kouki, J.: Understorey vegetation in spruce-dominated forests in eastern Finland and Russian Karelia: Successional patterns after anthropogenic and natural disturbances, *For. Ecol. Manag.*, 215(1–3), 113–137, doi:10.1016/j.foreco.2005.05.008, 2005.
- Wang, Z., Schaaf, C. B., Chopping, M. J., Strahler, A. H., Wang, J., Román, M. O., Rocha, A. V., Woodcock, C. E. and Shuai, Y.: Evaluation of Moderate-resolution Imaging Spectroradiometer (MODIS) snow albedo product (MCD43A) over tundra, *Remote Sens. Environ.*, 117, 264–280, doi:10.1016/j.rse.2011.10.002, 2012.
- 650 Wickham, H.: ggplot2: Elegant Graphics for Data Analysis, R, Springer-Verlag, New York. [online] Available from: <http://ggplot2.org>, 2016.

Wilcox, R. R.: Introduction to robust estimation and hypothesis testing, 4th edition., Elsevier, Waltham, MA., 2016.

WMO: Guidelines on the quality control of data from the World Radiometric Network, World Meteorological Organization, Leningrad. [online] Available from: [https://library.wmo.int/pmb\\_ged/wmo-td\\_258\\_en.pdf](https://library.wmo.int/pmb_ged/wmo-td_258_en.pdf), 1987.

655 Zhang, D.: rsq: R-Squared and Related Measures, R. [online] Available from: <https://CRAN.R-project.org/package=rsq>, 2018.

Zhang, Q., Wang, Y., Wu, Y., Wang, X., Du, Z., Liu, X. and Song, J.: Effects of Biochar Amendment on Soil Thermal Conductivity, Reflectance, and Temperature, *Soil Sci. Soc. Am. J.*, 77(5), 1478–1487, doi:10.2136/sssaj2012.0180, 2013.

660 Zhang, Y., Chen, H. Y. H. and Reich, P. B.: Forest productivity increases with evenness, species richness and trait variation: a global meta-analysis: Diversity and productivity relationships, *J. Ecol.*, 100(3), 742–749, doi:10.1111/j.1365-2745.2011.01944.x, 2012.

665

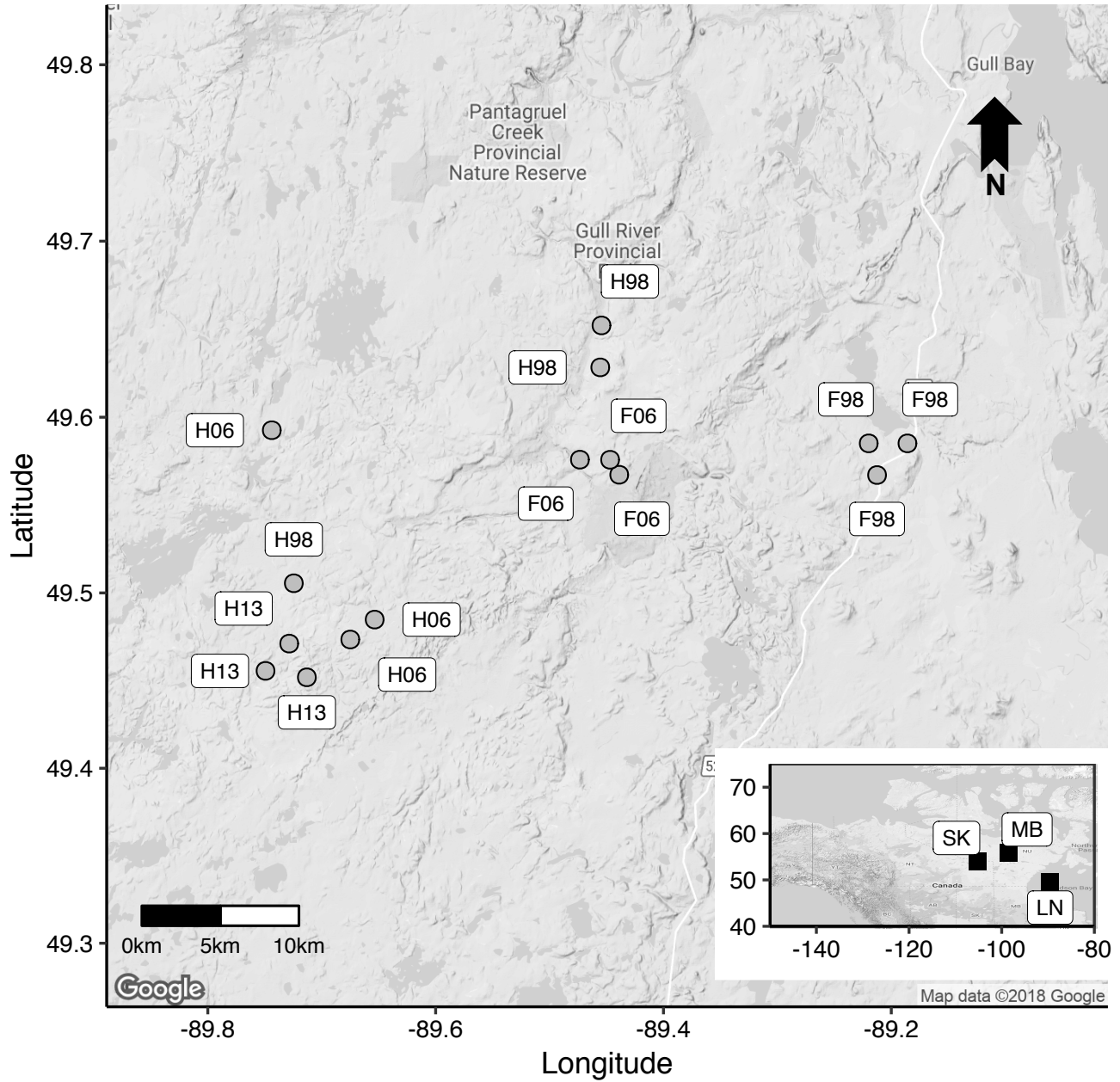
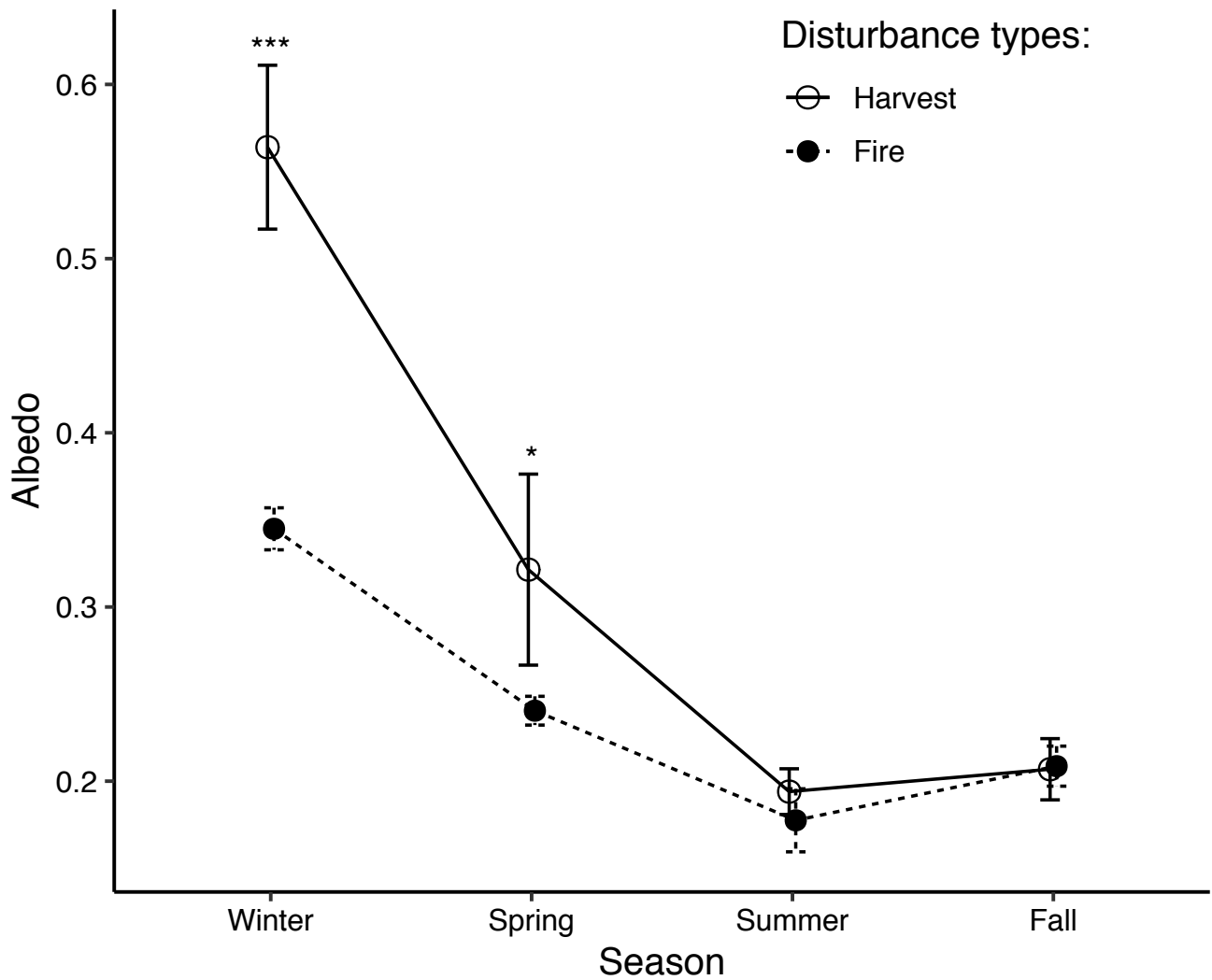


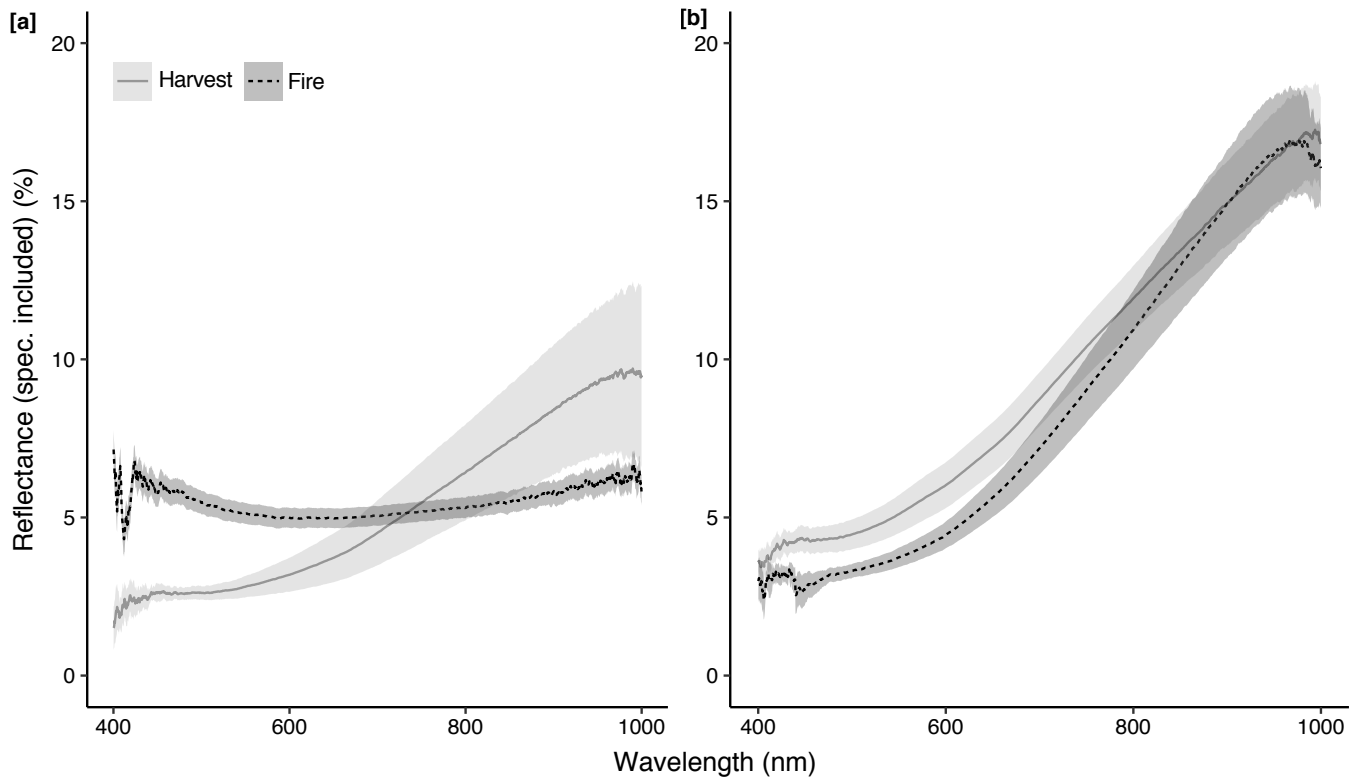
**Figure 1.** Map of the study area. Labels in the rectangular boxes indicate disturbance types (H: harvest and F: fire) and years (98: 1998, 06: 2006, and 13: 2013) for each plot (grey circles). **Inset:** black squares indicate locations of all data sources including the current study area (LN: Lake Nipigon area, Ontario, Canada; SK: Saskatchewan, Canada; MB: Manitoba, Canada).



675

**Figure 2.** Comparison of seasonal albedo (mean  $\pm$  SE) in post-harvest and post-fire stands. Winter (no. of observations for post-fire stands,  $n_F = 35$ ; no. of observations for post-harvest stands,  $n_H = 48$ ) and summer ( $n_F = 44$ ,  $n_H = 41$ ) albedo data were from 0–19-year-old stands, and spring ( $n_F = 30$ ,  $n_H = 30$ ) and fall ( $n_F = 30$ ,  $n_H = 30$ ) albedo data were from 7–19-year-old stands. Albedo of 0–6-year-old post-fire stands were from secondary sources. \* and \*\*\* indicate significant mean albedo differences between post-harvest and post-fire stands with  $p = 0.11$  and  $p < 0.01$ , respectively.

680



685 **Figure 3.** Specular-included ground surface reflectance (400–1000 nm) of post-harvest and post-fire stands. Lines indicate mean  
 685 reflectance (number of sample (n) × 10 replicated measurements/sample) in the corresponding wavelengths, and shades indicate SE. **[a]**  
 690 ground surface reflectance of young (4-year old) post-harvest stands (n = 9) and a post-fire stand (n = 12). **[b]** ground surface reflectance  
 695 of old (11- and 19-year old) post-harvest (n = 18) and post-fire (n = 18) stands.

690

695

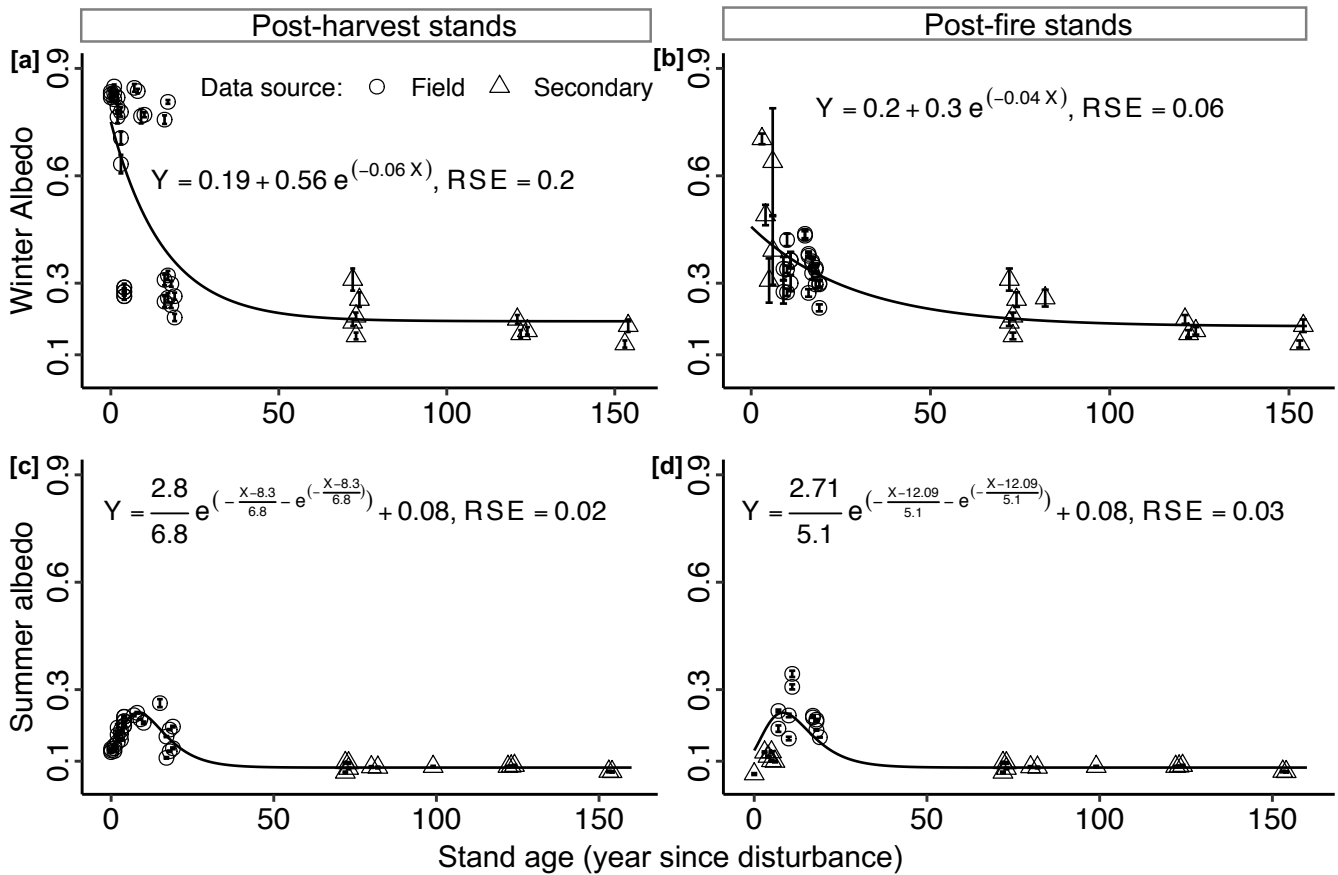


**Figure 4.** Stand age affecting mean seasonal albedo ( $\pm$  SE) in boreal forest over 0–150 years of stand development. Mean winter albedo as a function of stand age in **[a]** post-harvest stands ( $n = 42$ ) and **[b]** post-fire stands ( $n = 36$ ). Mean summer albedo as a function of stand age in **[c]** post-harvest stands ( $n = 41$ ) and **[d]** post-fire stands ( $n = 30$ ). Each field-data point is the average seasonal albedo (error bars indicate standard errors) of three plots from each stand-age category over the study period.

700

705

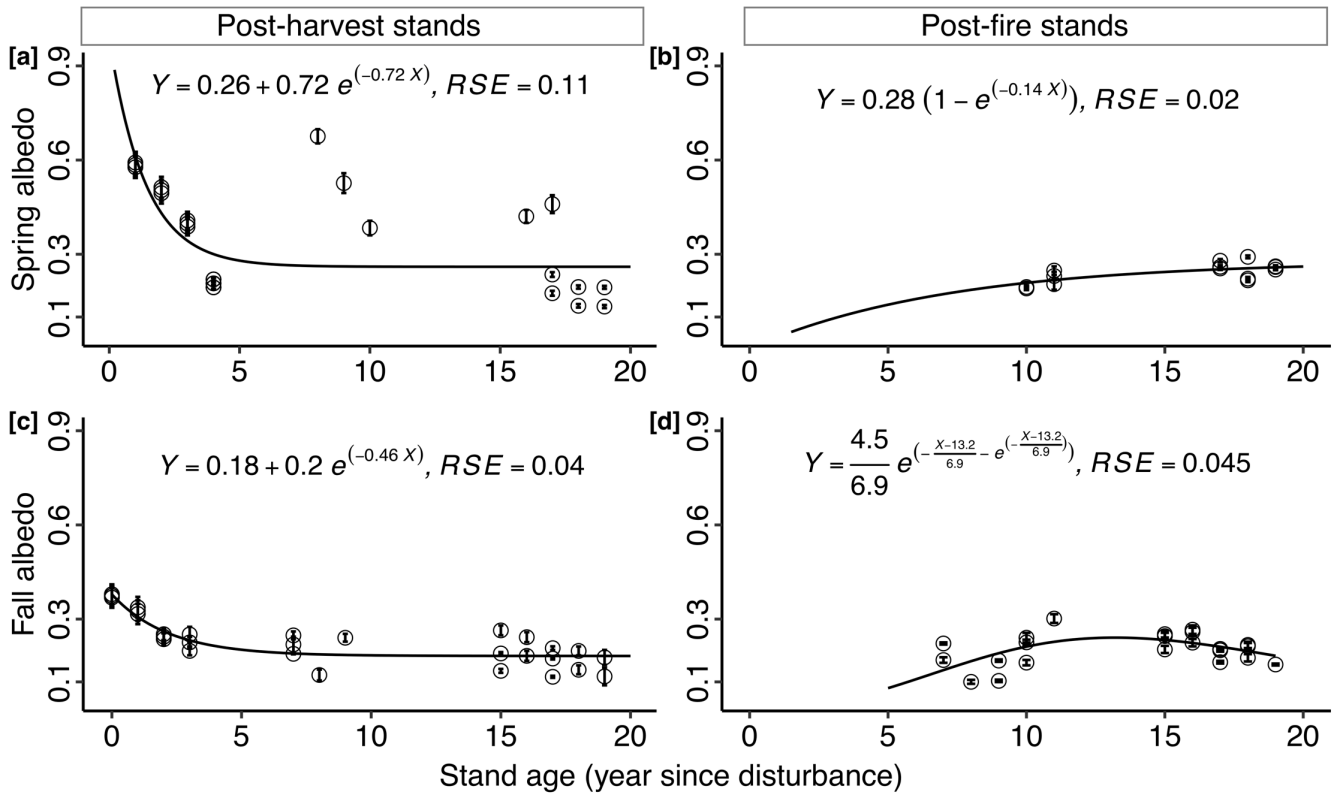
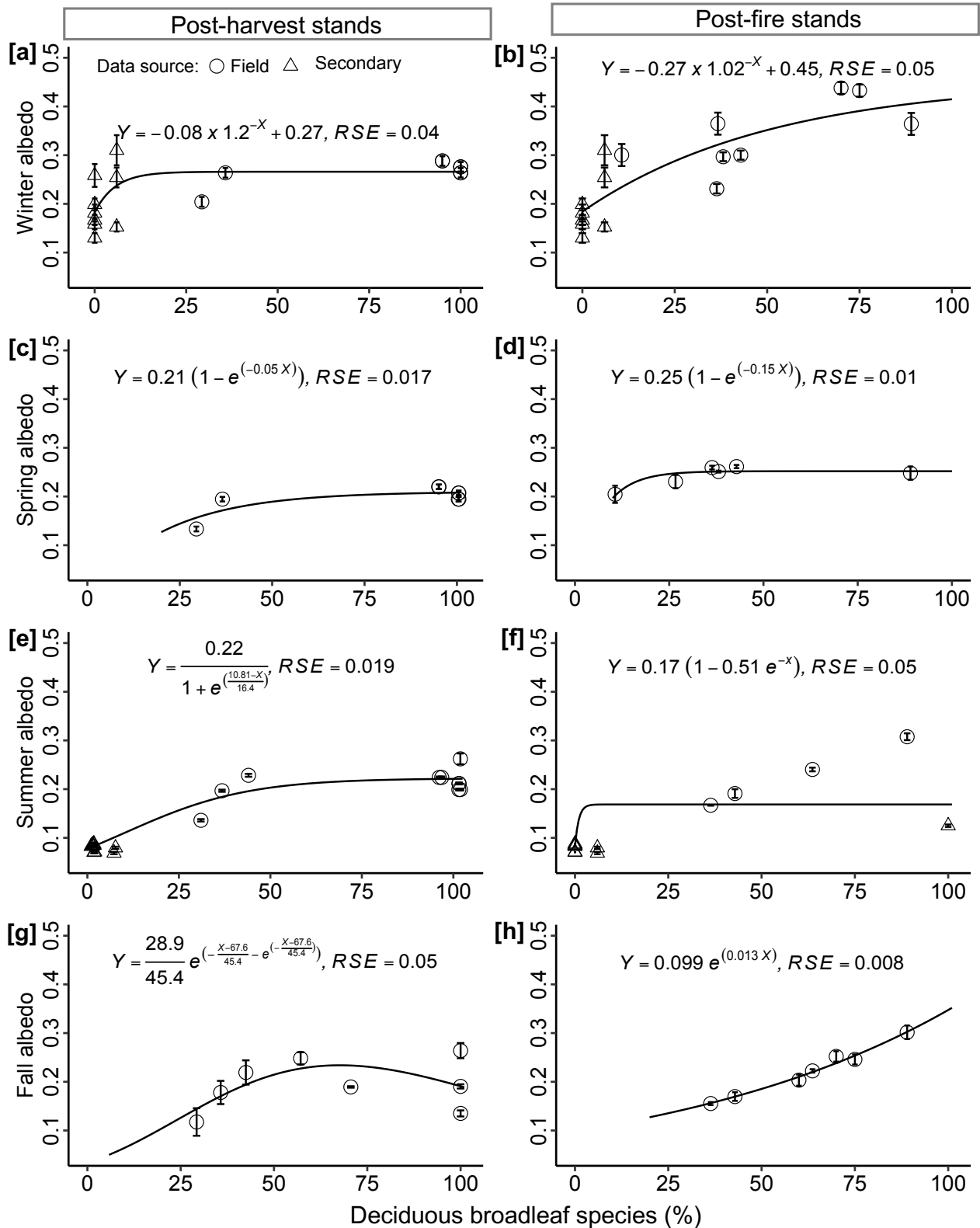


**Figure 5.** Stand age affecting mean seasonal albedo ( $\pm$  SE) in boreal forest in the early seral stage. Mean spring albedo as a function of stand age in **[a]** post-harvest stands ( $n = 26$ ) and **[b]** post-fire stands ( $n = 14$ ). Mean fall albedo as a function of stand age in **[c]** post-harvest stands ( $n = 29$ ) and **[d]** post-fire stands ( $n = 22$ ). Each field-data point is the average seasonal albedo (error bars indicate standard errors) of three plots from each stand-age category over the study period.

710

715

720



725 **Figure 6.** Mean seasonal albedo ( $\pm$  SE) as a function of deciduous broadleaf species (%) (proportion of deciduous broadleaf species) in the boreal forest. Proportion of deciduous broadleaf species affecting mean winter albedo in **[a]** post-harvest stands ( $n = 17$ ) and **[b]** in post-fire stands ( $n = 20$ ), mean spring albedo in **[c]** post-harvest stands ( $n = 8$ ) and **[d]** post-fire stands ( $n = 6$ ), mean summer albedo in **[e]** post-harvest stands ( $n = 20$ ) and **[f]** post-fire stands ( $n = 15$ ), and mean fall albedo in **[g]** post-harvest stands ( $n = 8$ ) and **[h]** post-fire stands ( $n = 7$ ).



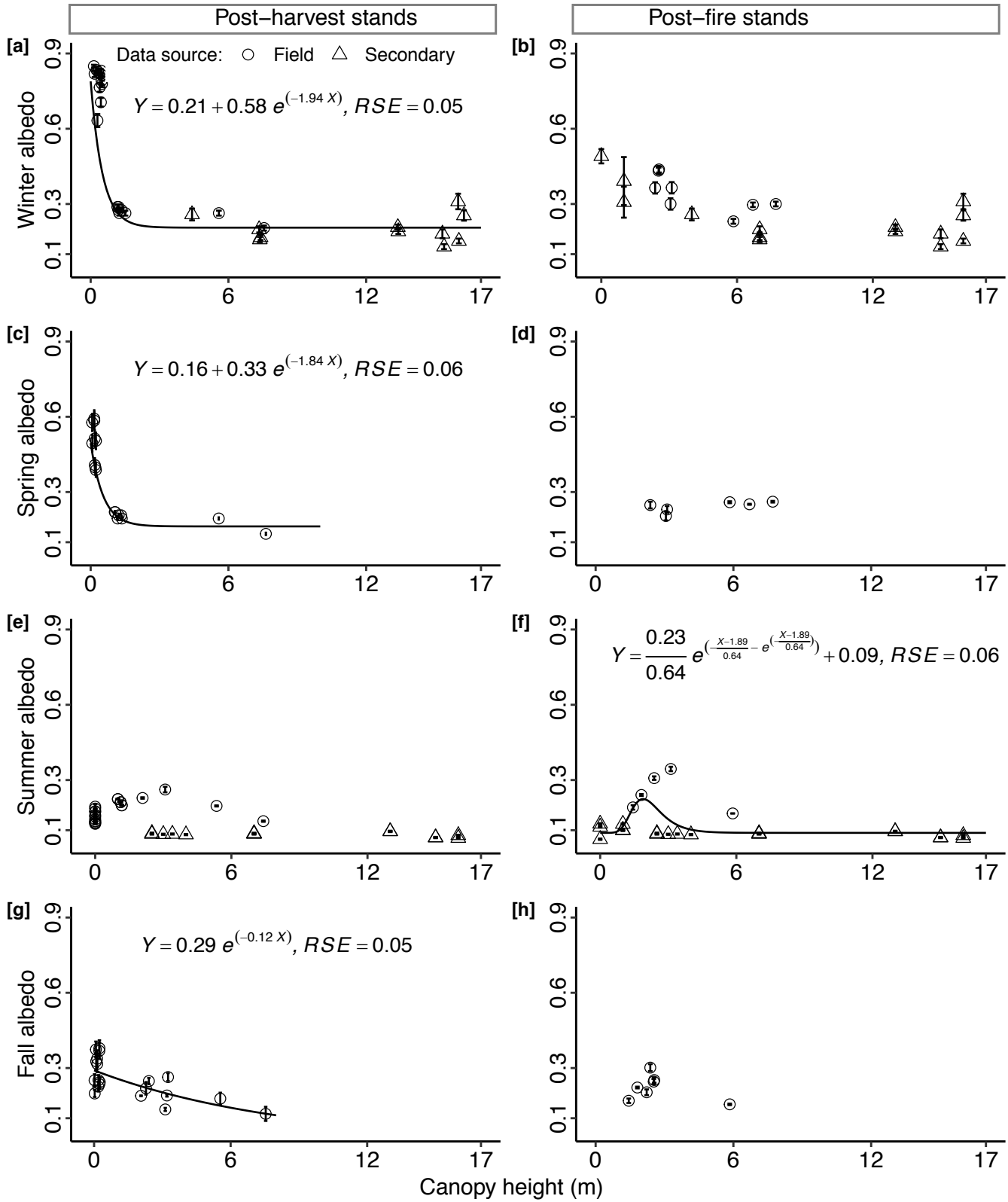


**Figure 7.** Mean seasonal albedo ( $\pm$  SE) as a function of canopy height (m) in the boreal forest. Canopy height affecting [a] mean winter albedo in post-harvest stands ( $n = 31$ ), [c] mean spring albedo in post-harvest stands ( $n = 16$ ), [f] mean summer albedo in post-fire stands ( $n = 23$ ), and [g] mean fall albedo in post-harvest stands ( $n = 20$ ). In [b, d, e, h] canopy height is not a significant predictor of the corresponding mean seasonal albedo; thus, no model is fitted to the data points.

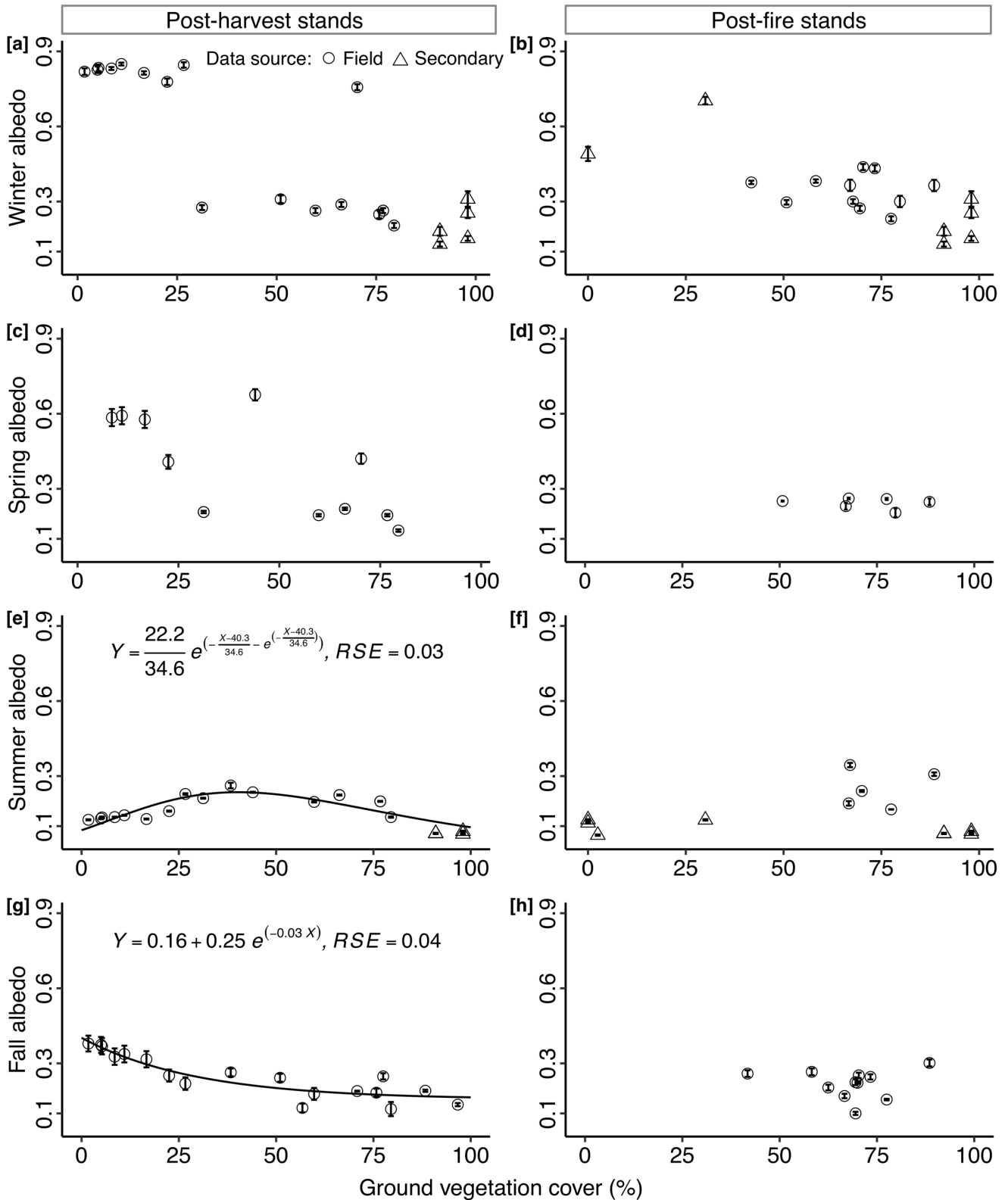


**Figure 8.** Mean seasonal albedo ( $\pm$  SE) as a function of ground vegetation cover (%) in the boreal forest. Ground vegetation cover affecting [e] mean summer albedo in post-harvest stands ( $n = 22$ ) and [g] mean fall albedo in post-harvest stands ( $n = 18$ ). In [a–d, f, h] ground vegetation cover is not a significant predictor of the corresponding mean seasonal albedo; thus, no model is fitted to the data points.

## 12.2 Tables

**Table 1. Structural characteristics of post-harvest and post-fire stands sampled. Mean values ( $\pm$  SE) are reported across all sites of a given disturbance type.**

745

Stand type	Stand age (year)	DBS (%)	LAI	Stem density (stems ha <sup>-1</sup> $\geq$ 5 cm DBH)	Height (m)	GCV (%)
Post-harvest	0–19	55.4 $\pm$ 11.2	0.4 $\pm$ 0.3	6472 $\pm$ 3060	1.7 $\pm$ 1.3	51.8 $\pm$ 20.1
Post-fire	7–19	37.8 $\pm$ 9.1	0.7 $\pm$ 0.4	8400 $\pm$ 1902	2.9 $\pm$ 1.5	62.5 $\pm$ 14.1

**Notes:** DBS, LAI, and GCV indicate deciduous broadleaf species (% by basal area), leaf area index, and ground cover vegetation.

750

755

760

765

770

775

780

785

**Table 2. Regression model coefficients and fit statistics for albedo as a function of stand attributes in different seasons in the boreal forest.**

Season	Post-harvest stands				Post-fire stands			
	Parameter Estimates		Model fit		Parameter Estimates		Model fit	
	Coefficient	Estimate	$\Delta AIC$	Adj. $R^2$	Coefficient	Estimate	$\Delta AIC$	Adj. $R^2$
Winter	Intercept	<b>1.722</b>			Intercept	<b>- 1.25</b>		
	SA	<b>- 0.031</b>			SA	- 0.004		
	PDBS	<b>- 0.021</b>	- 69.2	0.97	PDBS	<b>0.005</b>	- 5.3	0.75
	CH	<b>- 0.079</b>						
	SA:CH	<b>0.002</b>						
	PDBS:CH	<b>- 0.007</b>						
Spring	Intercept	<b>- 7.195</b>			Intercept	<b>- 1.747</b>		
	SA	<b>1.298</b>	- 495.4	0.99	SA	0.016	- 18.8	0.92
	PDBS	<b>0.116</b>			PDBS	0.002		
	CH	<b>- 1.264</b>						
	SA: PDBS	<b>- 0.024</b>						
Summer	Intercept	<b>- 1.377</b>			Intercept	<b>- 2.996</b>		
	SA	<b>0.032</b>	- 24.9	0.97	SA	<b>- 0.012</b>	- 48.3	0.95
	PDBS	<b>- 0.003</b>			PDBS	- 0.004		
	GVC	<b>- 0.01</b>			CH	<b>0.788</b>		
	SA: GVC	<b>- 0.0004</b>			SA: PDBS	<b>0.003</b>		
	PDBS: GVC	<b>0.0001</b>			SA: CH	<b>- 0.004</b>		
					SA:CH: PDBS	<b>- 0.001</b>		
Fall	Intercept	<b>0.398</b>			$\frac{4.5}{6.87} e^{(-\frac{SA-13.2}{6.87} - e^{-\frac{SA-67.62}{45.39}})}$	- 3.1	0.045 <sup>1</sup>	
	SA	0.013			$0.099 e^{0.013 PDBS}$			- 25.4
	CH	<b>- 0.182</b>	- 6.1	0.94				
	GVC	<b>- 0.007</b>						
	SA:CH	<b>0.007</b>						
	CH: GVC	<b>0.005</b>						
	SA:CH: GVC	<b>- 0.0002</b>						
	$\frac{28.86}{45.39} e^{(\frac{PDBS-67.62}{45.39} - e^{-\frac{PDBS-67.62}{45.39}})}$	- 0.9			0.049 <sup>1</sup>			

**Notes:** SA, PDBS, CH, and GVC indicate stand age (year), proportion of deciduous broadleaf species (%), canopy height (m), and ground vegetation cover (%), respectively. Parameter estimates for GLMs in bold and regular fonts indicate statistical significance at 1% and 5% level, respectively. For fall nonlinear regression models, 28.86 and 45.39 coefficients of post-harvest stands are significant at 5% level and the rest is significant at 1% level. <sup>1</sup> indicates residual standard error of the nonlinear regression model.  $\Delta AIC$  = AIC of the best-fit model – AIC of the corresponding null model.